necessary equations are obtained from: (1) the goemetrical relationship among G_o, Λ_1, and R; (2) evaluation of Equation (34) with $\Lambda_a = \Lambda_1$, and (3) evaluation of Equation (34) with $\Lambda_a = 1$.

In evaluating Equation (34) over the horizontal part of the profile, the slope $G'(\Lambda_1)$ is taken as the average of the slopes of the lines meeting at $\Lambda = \Lambda_1$, that is, $G'(\Lambda_1) = R/2$. When G_o and R are eliminated from these equations, Λ_1 is given by the implicit relation

$$\frac{1 - (3\Lambda_1^2 - \Lambda_1^3)^{-1}}{(7/8) - \Lambda_1 + (1/6)\,\Lambda_1^3 - (1/24)\,\Lambda_1^4} = B \qquad (36)$$

Numerical answers are obtained by evaluating B in Equation (36) for different input values of Λ_1. For a known set of Λ_1 and B, the quantity R is found, and the salinity ratio of interest becomes

$$S_h/S_{av} = [(3R/B) - 2]^{-1} \qquad (37)$$

The following tabulation gives the numerical results (slide rule accuracy):

B	Λ_1	R/B	S_h/S_{av}
0.074	0.66	0.994	1.020
0.177	0.67	0.986	1.042
0.284	0.68	0.980	1.070
0.509	0.70	0.961	1.130
1.154	0.75	0.926	1.282
2.02	0.80	0.897	1.447
5.97	0.90	0.845	1.887

It is seen that the Λ_1 values lie in the third of the film thickness which is closest to the free surface, and that the gradient of G at the free surface, R, is close to B and approaches B as B approaches zero.

Manuscript received February 23, 1965; revision received June 7, 1965; paper accepted June 8, 1965. Paper presented at A.I.Ch.E. Houston meeting.

Direct Contact Heat Transfer with Change of Phase:

Effect of the Initial Drop Size in Three-Phase Heat Exchangers

SAMUEL SIDEMAN, GIDEON HIRSCH, and YEHUDA GAT

Technion, Israel Institute of Technology, Haifa, Israel

The initial drop size of volatile fluids evaporating within immiscible, nonvolatile liquids was experimentally related to the overall heat transfer coefficient in single and multiparticle systems. Coalescence and turbulence diminish the effects of the initial size, which are thus limited to the lower part of the exchanger where single-drop characteristics are maintained. Condensation data of single bubbles are in good agreement with the single-drop relationship.

The problem of direct-contact heat exchangers was stimulated in the last decade by the quest for economic water desalination units. Of particular interest are the multiphase exchangers in the direct-contact freezing processes (*1* to *4*). Also of practical importance are the three-phase direct-contact exchangers where latent heat is transferred from the dispersed volatile fluid to a continuous nonvolatile, immiscible liquid (*5* to *8*). The obvious advantages of utilizing these multiphase exchangers are summarized elsewhere (*9, 10*), and attempts to ellucidate the transfer characteristics and the mechanism of heat transfer in such systems have been reported recently (*9* to *11, 13*).

The relationships between drop diameter and the heat transfer coefficient in direct-contact heat transfer systems without change of phase were reviewed recently (*12*). It was noted that, except at the transition zone between large (2 to 7 mm.) and small (below 1 to 3 mm.) drops, the heat transfer coefficient does not change appreciably with diameter of the drop. Nevertheless, a decrease of the transfer coefficient with increase in drop diameter was noted in a number of experiments, which is in accord with the classical theoretical derivations which predict the transfer coefficient to be inversely proportional to $d^{0.5}$.

Studies of single drops (*9*) and bubbles (*11*) evaporating and condensing, respectively, in stagnant, constant temperature, immiscible liquid media indicated a marked effect of the initial liquid drop diameter on the heat transfer coefficients. However, more information was needed before a quantitative relationship between these parameters could be attempted, and additional single-drop data

Samuel Sideman is at Oklahoma State University, Stillwater, Oklahoma, and Gideon Hirsch is at the Israel Atomic Energy Commission, Dimona, Israel.

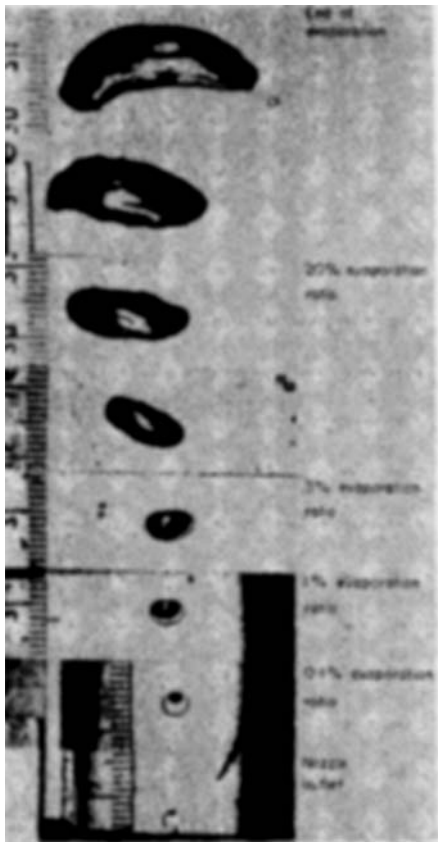

Fig. 1. Pentane drop evaporating in water. 3.5 mm. initial drop diameter. Picture taken with 16-mm. Paillard-Bolex H-16 movie camera (9).

were obtained with the apparatus described in reference 9. To gain insight into more realistic systems, a spray column was used to study the effects of interactions in multidrop systems. The practical implications are apparent, since the initial drop diameter may be a controlled variable in the experimental system.

SINGLE-DROP STUDIES

Overall Resistance to Heat Transfer

The calculation of the true overall heat transfer coefficient depends on the knowledge of the true, effective heat transfer area. As seen from Figure 1 in which a pentane drop is shown evaporating in water, it is quite difficult to determine the actual transfer area, even by assuming axial symmetry (which evidently is not the case). Also, and not least important, this method of calculations is laborious and tedious. Thus it is desirable to define a simpler criterion which will be independent of the intermediate deformations of the evaporating drop and will depend on measurable end values only. The latter are usually more readily and, more important, accurately measured.

Table 1. Overall Resistance Values for Various Initial Drop Diameters

	Pentane-sea water				Pentane-distilled water
d^*, mm. (average)	1.99	2.31	3.03	3.83	3.49
Average R	8.76	8.10	4.98	3.60	5.09
Variance	0.18			0.08	0.19
Variation coefficient	2%			2%	4%

The overall average resistance to heat transfer R was thus defined

$$R = t_v \Delta T / Q_{max} \qquad (1)$$

where $Q_{max} = \rho_d V_d L$ is the total amount of heat transferred to the evaporated drop. The time required for complete evaporation of the drop t_v is determined as the asymptotic value beyond which no volume change due to evaporation is noted.

The calculated values of R for the pentane-water systems are summarized in Table 1. Values for the ethyl chloride-distilled water system were calculated from the data of Klipstein (13). As seen in Figure 2, the values of R, in units of (sec.)(°C.)/cal., are related to the initial drop diameter d^* (mm.) by

$$R = B\, d^{*x} \qquad (2)$$

For the pentane-seawater system $B = 22.1$, $x = -1.36$ and for the ethyl chloride-distilled water system $B = 38.0$, $x = -2.07$.

Data for the pentane-distilled water, butane-seawater, and butane–24% sodium chloride solution (30) systems are limited to one-drop diameter, and only average values of R are presented in Figure 2 for comparison.

The Overall Heat Transfer Coefficient

The average heat flow rate $\bar{q}$ is related to the overall resistance to heat transfer by

$$\bar{q} = \frac{Q_{max}}{t_v} = \frac{\Delta T}{R} \qquad (3)$$

and can also be expressed in terms of the overall heat transfer coefficient and the transfer area. Unlike most conventional systems, the heat transfer area here varies

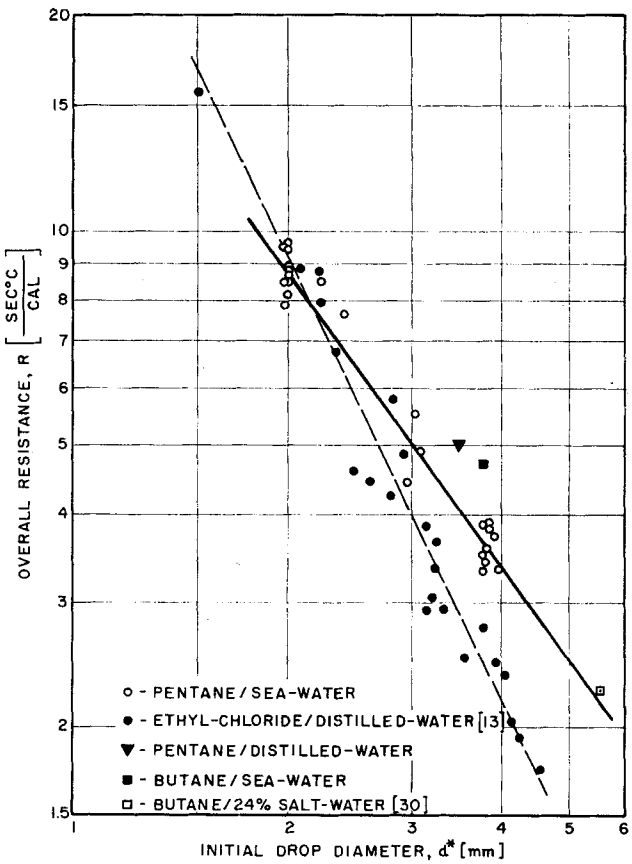

Fig. 2. Overall resistance as function of initial drop diameter.

during the evaporation process. The heat transfer coefficient must, therefore, be defined in relation to some conveniently determined area. Two cases follow.

Average transfer coefficient related to initial drop area The initial drop area A^* is determined relatively easily from pictures of the drops leaving the nozzle (or from correlations). The average heat transfer coefficient $\overline{U}^*$ related to the initial drop area A^* is defined by

$$\overline{q} = \overline{U}^* A^* \Delta T \tag{4}$$

From Equations (2) to (4)

$$\overline{U}^* = 1/RA^* C d^{*-(x+2)} \tag{5}$$

where $C = (\pi B)^{-1}$

For the pentane-seawater system

$$\overline{U}^* = 5.07 \times 10^4 d^{*-0.04} \tag{5a}$$

where $\overline{U}^*$ is expressed in kcal./(hr.)(sq. m.)(°C.) and d^* in mm.

For the ethyl chloride-distilled water system $B = 38$ and $\overline{U}^* = C d^{*0.07} \simeq 0.904$ cal./(sec.)(sq. cm.)(°C) = 3.26×10^4 kcal./(hr.)(sq. m.)(°C.).

These results are plotted in Figure 3 where the average values for the butane-seawater, pentane-distilled water, and butane-24% sodium chloride solution systems are also presented for comparison.

Average transfer coefficient related to average instantaneous area By analogy to Equation (4) the average heat transfer coefficient related to the average instantaneous total (vapor + liquid) contact area $\overline{A}$ is defined by

$$\overline{q} = \overline{U}\,\overline{A}\,\Delta T \tag{6}$$

Obviously, $\overline{U} = 1/R\overline{A}$. As will be discussed later, it is reasonable to assume that $\overline{A}$, the characteristic area, is directly proportional to the initial contact area, that is, proportional to d^{*2}. Equations (3) and (6) would thus yield

$$\overline{U} = C' d^{*-(x+2)} \tag{7}$$

where $C' = (\pi BW)^{-1}$ and W is the proportionality constant $\overline{A}/A^*$. Note that $\overline{U}\,\overline{A} = \overline{U}^* A^*$ and $\overline{U} = 1/R\overline{A} = \overline{U}^* A^*/\overline{A}$, and hence $C' = C/W$. As the value of $\overline{A}$ is unknown, the value of C' is obtained directly by plotting the experimental values of $\overline{U}$ vs. d^* as shown in Figure 3. For all the hydrocarbon systems, including some data of isopentane condensation in distilled water to be discussed below

$$\overline{U} = 3.7 \times 10^3 d^{*-0.04} \tag{7a}$$

For the pentane-seawater system

$$\overline{U} = 4.3 \times 10^3 d^{*-0.04} \tag{7b}$$

where $\overline{U}$ is given in kcal./(hr.)(sq. m.)(°C.) and d^* in mm. By comparing (7b) with (5a) one sees that $W = 11.8$. The characteristic average area $\overline{A}$ is thus 11.8 times larger than the initial area of the unevaporated drop or some 35% of the final bubble area of the completely evaporated drop. This is consistent with the smaller evaporation rates in the beginning of the evaporation process, where the internal resistance of the liquid in the drop is the controlling mechanism (*10*). The heat transfer coefficient related to initial area is thus about one order of magnitude greater than the one related to the average instantaneous total area. However, considering that the heat is transferred almost exclusively through the actual liquid-liquid surface (*9, 10, 13*), one can approximate (*10*) the true liquid-liquid heat transfer coefficient to be about 2.5 times the value of $\overline{U}$. It should be noted that $\overline{U}$ realized in these three-phase systems are larger by at least one order of magnitude than the surface heat transfer coefficients found in heat transfer studies with nonevaporating drops (*8, 9*).

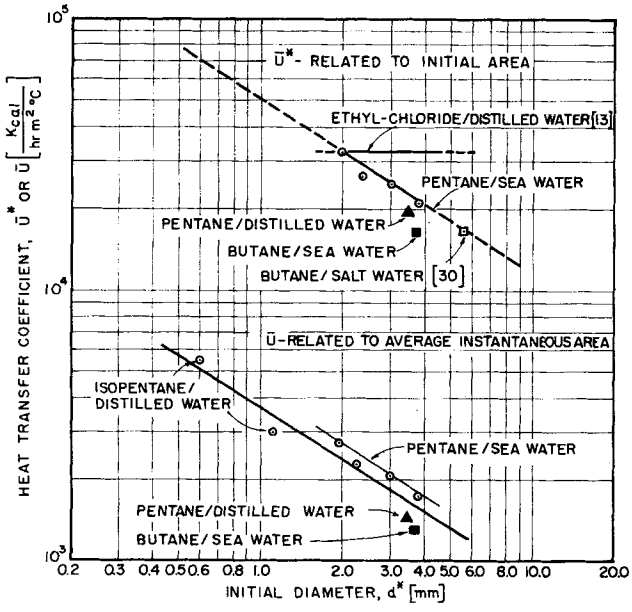

Fig. 3. Heat transfer coefficients as a function of initial drop diameter.

Discussion of Single-Drop Studies

As seen in Table 1, the variance of R is rather small, indicating the advantage of utilizing the overall resistance rather than the actual overall transfer coefficient. Whereas Q_{max} can be determined quite accurately from the pictures of the initial drops leaving the nozzle before evaporation starts, t_v, which is an asymptotic value, is determined less accurately. The error indicated by the variation coefficient in Table 1 is surprisingly small and practically unavoidable. In order to minimize errors due to the effect of hydrostatic head on the boiling temperature, only data where $\Delta T > 3$°C. were used here. However, since no effect of the temperature driving force on the heat transfer coefficient was noted (*9, 11*), the results undoubtedly are applicable in the practical interesting range of $\Delta T < 3$°C.

The proportionality assumed between $\overline{A}$ and d^{*2} may seem questionable in view of the continuous growth and deformation of the two-phase droplet which starts as a sphere and ends up as an ellipsoid or a spherical cap. The actual effective heat transfer area would therefore be expected to change continuously during the evaporation process. Also, the heat transfer mechanism changes from internal to external controlling resistance during the process (*10, 11*). However, the ratio of the effective liquid-liquid transfer area to the overall contact area was noted to vary only moderately during the evaporation process (*9*). Also, approximate calculation of the liquid-liquid contact area showed it to be proportional to the initial drop area (*13*), thus substantiating the above assumption.

The data for the ethyl chloride–distilled water system presented in Figure 2 indicate that the overall resistance is proportional to the initial diameter to the power of −2.07. This would indicate an exponent of 1.07 for the Reynolds group when reduced to the Nusselt vs. Reynolds relationship. Assuming experimental error, Kleipstein also assumed an exponent of 1.0 for the Reynolds number, indicating that the overall heat transfer coefficient $\overline{U}^*$, re-

lated to the initial areas of the drops, is independent of the initial drop diameter.

The different exponents obtained in these two studies most likely are due to the different physical properties of the systems, as well as the different nucleation techniques employed, rather than to different heat transfer mechanisms. The effect of the physical properties is seen by reference to the pentane-distilled water and the butane-seawater systems. The latter two systems exhibited identical transfer characteristics and yielded heat transfer coefficients which were quite close to the pentane-seawater system. However, some differences are evident in Figure 3. Since surface tension is the only physical property that differs appreciably between the pentane-seawater and the pentane-distilled water systems, it may be assumed that surface forces would play an important role in this evaporation process. Indeed, Klipstein noted strong effects of surfactants on the average heat transfer rate. Moreover, these effects differed appreciably for his small (~2 mm.) and large (~4 mm.) drops. Thus it is quite reasonable to expect some dependency of $\overline{U}^*$ on the initial drop diameter due to surface tension and excessive pressure due to curvature. These would effect higher temperature driving forces within the smaller drops and hence higher evaporation rates as compared with the larger ones.

As is well known, smaller drops are less susceptible to nucleation. In our study nucleation was sometimes induced by allowing minute amounts of air (or nitrogen) to dissolve in the volatile liquid, and/or by artificially introducing very small (below 0.1 mm.) nitrogen gas bubbles into the continuous water medium. Nevertheless, nucleation could not be induced in 2 mm. pentane drops in distilled water. These smaller drops ascended to the top of the column, where spontaneous evaporation into the gaseous phase took place. (Addition of sodium chloride to the water facilitated nucleation of these droplets, but no data are available.) With smaller drops of approximately 1 mm. diameter in seawater, nucleation was found erratic, starting anywhere along the column. Spontaneous, explosive evaporation was seen but all efforts to date to capture the evaporation process of these small drops on film were unsuccessful. Klipstein, on the other hand, induced nucleation in the ethyl chloride drops by supplying a sharp power pulse to the drops by discharging a condenser through a nichrome heating wire which was in contact with the drop at the nozzle. This electric pulse may have offset the internal pressure which affects natural nucleation, or at least affected the initial, slowest evaporation process.

Although the data were taken after the onset of nucleation, it is quite reasonable that part of the difference in the results of these two studies was due to the technique employed, especially since it affected the initial, slowest stages of the evaporation process. It is evident that more work is required to clarify these effects.

Since relatively low temperature differences (up to 15°C.) were used in this study, subcooling or superheating effects which may have existed would hardly affect Q_{max}, and did not affect the instantaneous heat transfer coefficients (*9*).

The study of condensation of single isopentane bubbles (*11*) in distilled water provides some means of verifying that Equations (*5a*), (*7a*), or (*7b*) may be extrapolated to smaller drops diameters. However, the transfer characteristics associated with the condensation process do not allow direct evaluation of t_v and hence the overall resistance, as defined by Equation (1). This is due mainly to the fact that condensation starts during the bubble formation period and the exact liquid content in the bubble leaving the nozzle is unknown. Moreover, condensation was never complete at the relatively low temperature range (up to 3°C.) used in these studies. Nevertheless, a reasonable comparison can be made between the overall transfer coefficients calculated by Equation (*7a*) and the transfer coefficients obtained from direct measurements of consecutive pictures of the rising condensing bubbles. The condensation coefficients reported here represent the main condensation range, where some 80% of the vapor mass condensates. The agreement is quite satisfactory, since the condensation data fall within ± 15% of the values extrapolated by Equation (*7a*). In view of the general similarity of the transfer mechanism of the evaporating drops and the condensing bubbles, Equation (*7a*) seems to be applicable practically in the range of 0.6 to 5.5 mm. initial liquid drop diameter.

The relationship between the overall transfer coefficient and the initial diameter obtained here differs somewhat from the earlier theoretical derivation of Sideman and Taitel (*9*), in which the external transfer coefficient was found to be proportional to the −0.5 power of the instantaneous equivalent (spherical) diameter of the two-phase drop. However, in deriving that relationship, they assumed the internal transfer coefficient to be negligible, whereas the overall resistance defined here includes the initial evaporation stages without neglect of the internal resistance. It is evident that though the external resistance plays a major role in the overall resistance, the effects of the internal resistance (especially at the beginning of the evaporation process) are not negligible.

SPRAY-COLUMN STUDIES

The Initial Drop Diameter

Unlike single-drop studies, where the surface transfer coefficient can be determined, spray columns are usually characterized by the overall volumetric transfer coefficient. This allows independence of the actual drop diameter, as very little information is usually available on drop diameters in spray columns. Even the two principal single orifice studies (*14, 15*) of drop formation in liquid-liquid systems differ in the basic characteristics of drop diameter as a function of the velocity in the orifice. However, investigations (*16, 18*) in connection with extraction in spray columns of clouds of drops at low flow rates of the dispersed phase gave results which roughly agree with Hayworth and Treybal's (*14*) correlation. At higher orifice velocities the liquid leaves the orifice in the form of a jet which subsequently breaks up into drops. Here, too, the drop size was found to agree (*19* to *21*), within order of magnitude, with the extrapolated Hayworth and Treybal's correlation.

In spite of the inaccuracy anticipated in using Hayworth and Treybal's correlation for the particular nonisothermal three-phase system discussed here, the calculated drop diameters presented in Table 2 are in general agreement with our observations and measurements. Attempts to determine the initial drop diameter in our system accurately by photographic techniques were unsuccessful due to the presence of partially evaporated drops and entrained vapor bubbles in the bottom part of the column. However, pictures and observations indicate that the calculated diameters are larger than the actual ones, which is in agreement with earlier observations (*21*). It is estimated that the calculated values are about 25 to 30% larger for the small droplets and some 40% larger than the larger ones.

In view of the error involved in using the calculated diameter as the independent variable, the orifice diameter was used in the graphical presentation of the data. It is important to note that the dispersed phase flow rate

TABLE 2. EXPERIMENTAL VARIABLES, SPRAY-COLUMN STUDY

	Series	B	E	F
Orifice diameter	D, mm.	0.5	1.5	2.5
No. of orifices	n	12	5	5
Orifice cross area	a, sq. mm.	0.196	1.765	4.91
Total cross area	A, sq. mm.	2.35	8.83	24.55
Orifice velocity	u, cm./sec.	65.3	19.4	6.25
Initial drop diameter calculated (*14*)	d^*, mm.	1.65	5.02	6.1

was constant in all the runs presented here. The velocities and diameters of the orifices were so chosen that operation was always close to the jetting point. This assured more uniformity of the drop diameters. It was noted that the density of the drops near the distributing plate was different for the different orifices used. The smaller the orifice, the smaller the droplets and the greater the apparent concentration of the dispersed droplets at the bottom of the column.

Experimental

A detailed description of the apparatus is presented elsewhere (*8*).

In the runs reported here the pentane flow rate was 56.1 g./min. or 1.44 cu. m./(hr)/(sq. m.) (column cross section). The water outlet approach temperature ΔT_2 was kept constant at about 1.7°C. for all runs, while the water flow rate was varied. Three ebonite disks were used, 3 mm. thick. The characteristics of the disks are included in Table 2.

Spray-Column Results and Discussion

The droplets leaving the nozzles at the bottom evaporated and grew while rising in the column and two major operating zones were seen in the column: a free rising zone and a turbulent zone. A third and at present less significant zone was a relatively small foam zone on top of the turbulent zone. In general, these two major zones are comparable to the streamline and turbulent regions noted in gas-liquid contacting columns (*22*) at different gas flow rates. In the lower part of the column, the streamline region of low holdup, the evaporating droplets rose essentially unhindered. As the superficial vapor velocity increased with vapor generation, the growing droplets lost their identity at the upper part of the column. Obviously, interfacial area decreases with increased coalescence in the turbulent zone.

The optimal column height is defined here as the height of the column above which evaporation of the dispersed phase is complete. This point corresponds to the optimal column volume and the maximum volumetric transfer coefficient at the given temperatures and flow rates. It is sufficient to note that the optimal height is determined experimentally by varying the column height, while inlet conditions remain constant.

The effect of the various orifice diameter on the optimal column height at various water flow rates is shown in Figure 4. The optimal height is clearly affected by the different disks. The larger the orifice diameter, corresponding to larger initial drop diameters, the larger the required optimal height. This is in complete agreement with Sideman and Taitel's single-drop studies (*9*) where the height of evaporation increased with increasing initial drop diameter. It is also consistent with Keith and Hixon (*19*) who noted that coalescence was promoted by increasing nozzle size and therefore by increasing drop size. Smaller droplets have less tendency to coalesce, whereas oscillations and vibrations of the larger drops increase the change of contact and enhance coalescence. Increased coalescence would decrease the effective heat transfer area per unit volume, increase optimal height, and decrease the volumetric transfer coefficient. The effect of the continuous phase flow rate on the optimal column height is rather slight. It is however more significant with larger drops, since increasing the continuous phase flow rates increases holdup and hence coalescence (*16*).

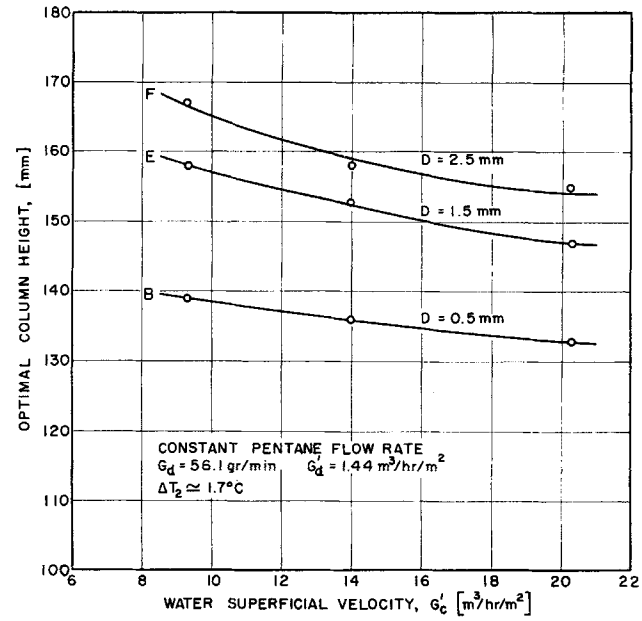

Fig. 4. Optimal column height as a function of water superficial velocity for three different pentane distributing plates.

The effect of the various disks on the volumetric transfer coefficient as a function of the water flow rate is shown in Figure 5. In view of the definition of the volumetric transfer coefficient ($U_v = Q/\Delta T_{ln} V$), the trend is obvious. The smaller the droplets the smaller the optimal volume and the larger the volumetric transfer coefficient.

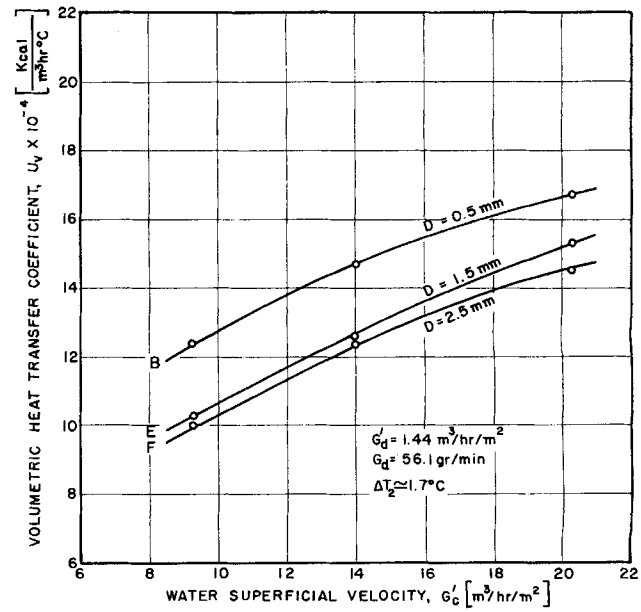

Fig. 5. Volumetric heat transfer coefficient as a function of water superficial velocity for three pentane distributing plates.

The results obtained indicate an advantage in operating with small size droplets in this three-phase heat exchanger at a given flow rate. This is consistent with a recent study (*23*) of the effects of mixing on the three-phase system. The heat transfer rate was found to increase with an increase of the power input to the mixer. The smaller evaporating drops thus obtained yielded larger heat transfer area per unit volume as well as larger transfer coefficients. No nucleation problems were noted in the agitated system. Some effects of nucleation were noted in the startup period of the spray column, but disappeared once operation was under way (*8*).

An approximate relationship between the initial diameter and the volumetric heat transfer coefficient may be obtained by plotting (Figure 6) the latter against the calculated drop diameter given in Table 2 for various water flow rates. This yields

$$U_v \sim d^{*-y} \qquad (8)$$

where y is 0.135, 0.128, and 0.1 for water flow rates of 9.3, 14.0, and 20.3 cu. m./(hr.)(sq. m.), respectively. Obviously, the dependency is not too strong.

It is noteworthy that liquid-liquid spray-column exchangers, as well as gas-liquid contacting systems, were found to be only slightly, if any, affected by orifice diameter (*24, 27*) at high holdup ratios. In liquid-liquid systems with relatively dense population of drops, drop diameter increases with increasing holdup (which in turn depends on dispersed phase flow rate) and decreasing relative (slip) velocity. Nevertheless, the transfer area per unit volume increases with the holdup and the volumetric transfer coefficient increases despite the increase of the diameter of the drop. As flooding or desired near-flooding conditions are approached, the drop diameter for a given two-liquid system is a function of flow rates, holdup (and hence slip velocity), and temperature, rather than of the orifice diameter.

A generally similar situation, though much more complicated, exists in gas-liquid contacting system (*27*). "The stable bubble size also depends on the level of turbulence existing in the continuous phase, and this level will, of course, be higher as the orifice diameter is decreased with consequent increase in energy dissipation, observed as pressure drop." Hence, "small bubbles which may be initially formed from fine orifices eventually coalesce to larger ones, the ultimate size being determined by the turbulent level" (*26*). However, the smaller the gas flow rate the smaller the apparent turbulence and the larger the effect of the initial bubble size on the volumetric transfer coefficient. It is relevent to note that the volumetric mass transfer coefficient in the turbulent region of gas-liquid contacting systems (*22*) was found to be independent of the gas flow rate. Also, a strong dependency of the mass transfer coefficient on the volume fraction of the dispersed phase was noted (*28*) at low volumetric holdups.

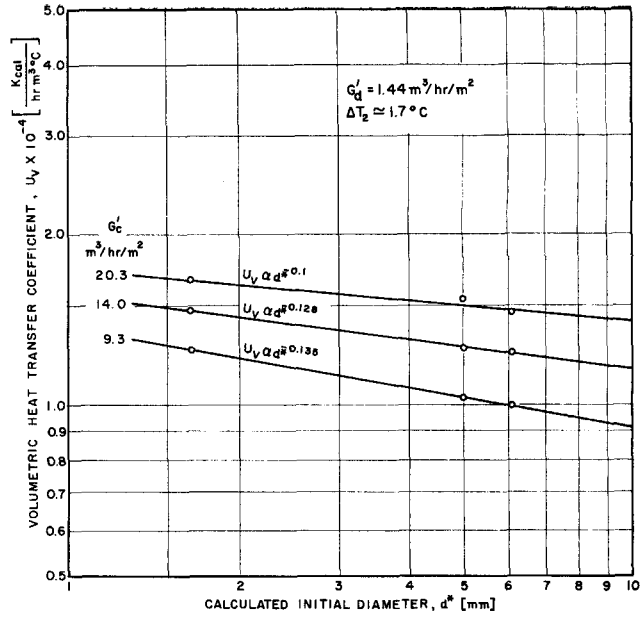

Fig. 6. Volumetric heat transfer coefficients as a function of the calculated initial drop diameter at various water flow rates. G'_d = 1.44 cu. m./(hr.) (sq. m.). $\Delta T_2 \simeq 1.7$.

Although dispersed phase flow rate was not varied in the work reported here, the superficial velocity did change along the column. It is thus reasonable to assume that the effect of drop size is mainly limited to the free rising streamline zone at the lower part of the column. The upper turbulent zone, being analogous to a gas-liquid system at high gas flow rates, is practically unaffected by the initial particle size. This is consistent with the independence of the gas holdup on orifice diameter, and hence bubble size, at high gas flow rates (*29*) and the weak dependence of the holdup on the continuous phase flow rate (*22*). It is, therefore, reasonable to expect that as the dispersed phase flow rate and superheat (*8*) increases, and the free rise zone decreases due to increased turbulence and coalescence, the effect of the initial diameter on the optimal height and volumetric transfer coefficient will diminish. It is, however, important to note that the dispersed phase flow rate used here corresponds to the maximum volumetric coefficient obtained in this system.

TABLE 3. SOME REPRESENTATIVE EXPERIMENTAL DATA

Run	Flow rate: Pentane, G_d, g./min.	Flow rate: Water, G_c, kg./min.	Flow ratio, $\frac{G_d}{G_c} \times 100$, wt. %	Superficial velocity: Water, G_c', cu. m./(hr.)(sq. m.)	Superficial velocity: Pentane, G_d', cu. m./(hr.)(sq. m.)	Orifice velocity, u, cm./sec.	Inlet temperature, Tc_1, °C.	Approach temperature, ΔT_2, °C.	Log-mean temperature, $(\Delta T)_{ln}$, °C.	Optimal height, Z opt., mm.	Vol. transfer coefficient, $U_v \times 10^{-3}$, kcal./(cu. m.)(hr.)(°C.)
B11	56.1	0.591	9.49	9.29	1.46	65.3	45.9	1.7	4.6	139	124
B12	56.0	0.890	6.3	14.0	1.44	65.2	—	1.7	—	136	(147)
B13	56.1	1.295	4.33	20.3	1.44	65.3	41.27	1.75	3.2	133	167
E11	55.8	0.592	9.43	9.3	1.43	17.25	45.85	1.7	4.70	158	103
E12	57.1	0.893	6.37	14.0	1.47	17.65	43.15	1.8	3.9	153	126
E13	55.5	1.295	4.29	20.3	1.425	17.17	41.2	1.7	3.15	147	153
F11	55.7	0.592	9.41	9.3	1.43	6.20	45.85	1.7	4.65	167	100
F12	56.2	0.890	6.31	14.0	1.44	6.25	42.95	1.7	3.8	158	124
F13	56.5	1.295	4.36	20.3	1.45	6.29	41.2	1.8	3.20	155	145

CONCLUSIONS

The initial drop diameter of pentane droplets evaporating within an immiscible water medium was found to affect the overall heat transfer coefficients. The smaller the droplets the larger the transfer coefficients. Surface tension and excessive pressure to the curvature seem to play an important role.

Studies of single pentane drops evaporating in seawater revealed that the overall surface heat transfer coefficient depends on the initial droplet diameter to the −0.64 power. This is consistent with the −0.5 power found earlier for the instantaneous transfer coefficient where internal resistance was assumed negligible. Data for our preliminary studies of condensation of single bubbles are in general agreement with the relationship obtained.

Countercurrent spray-column studies conducted at constant dispersed phase flow rates but with orifices of different diameters substantiated the above conclusions. Smaller orifices, associated with faster orifice velocities and smaller droplets, required lower optimal column heights and yielded higher volumetric heat transfer coefficients.

ACKNOWLEDGMENT

The financial support of the Israel National Council for Research and Development during the experimental part of this work is gratefully acknowledged. This report was written while one of the authors (S.S.) was a visiting professor at the School of Chemical Engineering at Oklahoma State University, Stillwater, Oklahoma, on a National Science Foundation Senior Foreign Scientist Fellowship. The cooperation of the N.S.F. and O.S.U. is highly appreciated.

NOTATION

a = cross area of single orifice
A = orifice cross area, total
A^* = area of initial drop
$\overline{A}$ = average of total heat transfer area
B = constant
C = constant
C' = constant
D = diameter, orifice
d^* = initial drop diameter, mm.
G = mass flow rate
G' = superficial velocity (in column)
L = latent heat of evaporation
n = number of orifices
Q_{max} = total heat transferred to drop, cal.
q = rate of heat transfer in column
q = average rate of heat transfer, Q_{max}/t_v
R = overall resistance to heat transfer, (sec.)(°C.)/cal.
T = temperature
ΔT = average temperature difference between drop and water
ΔT_2 = approach temperature, liquid exit
ΔT_{ln} = log mean temperature difference
t_v = time of complete evaporation of drop
U^* = average overall heat transfer coefficient, related to initial contact area
$\overline{U}$ = overall average heat transfer coefficient, related to characteristic average of total area
$\overline{U_v}$ = volumetric heat transfer coefficient
u = velocity in orifice
V_d = volume of drop
V = optimal volume of column
W = ratio of average to initial contact area, $\overline{A}/A^*$
x = exponent, Equation (2)
y = exponent, Equation (8)
Z = optimal column height
ρ = density

Subscripts

1 = continuous phase inlet
2 = continuous phase outlet
c = continuous phase
d = dispersed phase
v = volumetric

LITERATURE CITED

1. Weigandt, H. F., *Publ. 568, 377,* Natl. Acad. Sci., Washington, D. C. (1958).
2. Umano, S., *Japan. Govt. Chem. Ind. Res. Publ.,* in English (May, 1959).
3. Weigandt, H. F., *O.S.W. Progr. Rept. No. 41* (August, 1960).
4. Karnofsky, G., and P. F. Stienhoff, *O.S.W. Progr. Rept. 40* (July, 1960).
5. Lackey, D. L., M.S. thesis, Univ. California, Berkeley (1961).
6. Wilke, C. R., C. T. Cheng, V. L. Ledesma, and J. W. Porter, *Univ. California, Berkeley Sea Water Conversion Lab., Rept. No. 63-6* (August, 1963); *Chem. Eng. Progr.,* **59,** No. 12, 69 (1963).
7. Harriott, Peter, and H. F. Wiegandt, *A.I.Ch.E. J.,* **10,** 5, 755 (1964).
8. Sideman, Samuel, and Yehuda Gat, *Technion Res. Develop. Found. Ltd., Proj. CE-16, No. 10* (December, 1964); presented at A.I.Ch.E. Minneapolis Meeting (September, 1965).
9. Sideman, Samuel, and T. Taitel, *Intern. J. Heat Mass Trans.,* **7,** 1273 (1964).
10. Sideman, Samuel, and Gideon Hirsch, *Israel J. Technol.,* **2,** 234 (1964).
11. ————, *A.I.Ch.E. J.,* **11,** No. 6, 1019 (1965).
12. Sideman, Samuel, and H. Shabtai, *Can. J. Chem. Eng.,* **42,** No. 3, 107 (1964); **42,** No. 5, 238 (1964).
13. Klipstein, D. H., D.Sc. thesis, Massachusetts Inst. Technol. (June, 1963).
14. Hayworth, C. B., and R. E. Treybal, *Ind. Eng. Chem.,* **42,** 1174 (1950).
15. Null, H. R., and H. F. Johnson, *A.I.Ch.E. J.,* **4,** 273 (1958).
16. Sherwood, T. K., J. E. Evans, and J. V. Longcor, *Ind. Eng. Chem.,* **31,** 1144 (1939).
17. Licht, W., and J. B. Conway, *Ind. Eng. Chem.,* **42,** 1151 (1950).
18. West, F. B., A. P. Robinson, A. C. Morgenthaler, T. R. Beck, and D. K. McGregor, *Ind. Eng. Chem.,* **42,** 234 (1951).
19. Keith, F. W., Jr., and A. N. Hixson, *Ind. Eng. Chem.,* **47,** 258 (1955).
20. Jackson, R., *Chem. Eng.,* **CE-107** (May, 1964).
21. Garwin, L., and B. D. Smith, *Chem. Eng. Progr.,* **49,** No. 11, 591 (1953).
22. Shulman, H. L., and M. C. Molstad, *Ind. Eng. Chem.,* **42,** 1058 (1950).
23. Sideman, Samuel, and Zvi Barsky, *A.I.Ch.E. J.,* **11,** No. 3, 539 (1965).
24. Thompson, W. S., T. Woodward, W. A. Shrode, E. D. Baird, and D. A. Oliver, *Office of Saline Water Progr. Rept. No. 63* (April, 1962).
25. Minard, G. W., and A. I. Johnson, *Chem. Eng. Progr.,* **48,** No. 2, 62 (1952).
26. Calderbank, P. H., *Brit. Chem. Eng.,* **1,** 206 (1956).
27. Bridge, A. G., Leon Lapidus, and J. C. Elgin, *A.I.Ch.E. J.,* **10,** No. 6, 819 (1964).
28. Setzer, H. J., and R. E. Treybal, paper presented at A.I.Ch.E. Houston meeting (December, 1963).
29. Quigley, C. J., A. I. Johnson, and B. L. Harris, *Chem. Eng. Progr. Symposium Ser. No. 16,* **51,** 31 (1955).
30. Canning, F. T., personal communication (June, 1965).

Manuscript received March 5, 1965; revision received July 10, 1965; paper accepted July 26, 1965. Paper presented at A.I.Ch.E. Los Angeles meeting.